IJNAOE
©SNAK, 2014

Int. J. Nav. Archit. Ocean Eng. (2014) 6:27~38
http://dx.doi.org/10.2478/IJNAOE-2013-0161
pISSN: 2092-6782, eISSN: 2092-6790

Effect of static mixer geometry on flow mixing and pressure drop in marine SCR applications

Taewha Park[1], Yonmo Sung[1], Taekyung Kim[1], Inwon Lee[2], Gyungmin Choi[3] and Duckjool Kim[3]

[1]*Graduate Program, School of Mechanical Engineering, Pusan National University, Busan, Korea*
[2]*Global Core Research Center for Ships and Offshore Plants, Pusan National University, Busan, Korea*
[3]*Pusan Clean Coal Center, Pusan National University, Busan, Korea*

ABSTRACT: *Flow mixing and pressure drop characteristics for marine selective catalytic reduction applications were investigated numerically to develop an efficient static mixer. Two different mixers, line- and swirl-type, were considered. The effect of vane angles on the relative intensity, uniformity index, and pressure drop was investigated in a swirl-type mixer; these parameters are dramatically affected by the mixer geometry. The presence of a mixer, regardless of the mixer type, led to an improvement of approximately 20% in the mixing performance behind the mixer in comparison to not having a mixer. In particular, there was a tradeoff relationship between the uniformity and the pressure drop. Considering the mixing performance and the pressure drop, the swirl-type mixer was more suitable than the line-type mixer in this study.*

KEY WORDS: Selective catalytic reduction; Static mixer; Uniformity index; Pressure drop; Marine diesel engine.

INTODUCTION

In order to meet stringent future emission regulations from the environmental protection agency (EPA), especially with respect to reducing nitrogen oxides (NO_x), various technologies such as basic internal engine modifications, fuel switching, direct water injection, exhaust gas recirculation (EGR), and selective catalytic reduction (SCR) have been recommended for marine diesel engines. The international maritime organization (IMO) has regulated NO_x emissions from marine vessels. The IMO's Tier III standard requires that marine vessels must reduce NO_x emissions by 80% between 2010 and 2016 (DieselNet, 2008). SCR is one of the most promising technologies for accomplishing this aggressive regulation. As a reducing agent, urea is preferred in marine SCR applications because of its safety and low toxicity. Urea water solution (UWS), containing 32.5*wt%* urea, is injected into the hot gas stream from exhaust manifolds, and then, NH_3 is generated by dewatering, thermolysis, and hydrolysis processes. The urea-SCR reactor should be controlled to ensure high de-NO_x performance, low NH_3 slip, and low urea consumption. To maximize the de-NO_x efficiency and minimize the NH_3 slip, a controlled turbulent mixing process for two-phase flow, such as UWS with the exhaust gas stream, and a highly uniform flow in front of the SCR reactor must be obtained.

Flow mixing is a common device unit operation in a large number of processes, and it is used in many different applications

Corresponding author: *Gyungmin Choi*, e-mail: *choigm@pusan.ac.kr*

where a defined degree of homogeneity of a fluid is desired (Regner et al., 2006). In particular, a mixing device, e.g., a static mixer is usually installed to improve the rate of decomposition for urea to NH_3 and to enhance the uniformity of the spatial distribution of NH_3 and isocyanic acid (HNCO) (Munnannur and Liu, 2010). However, the increase in the system pressure drop because of mixing must be minimized.

There have been many attempts to develop static mixers for mobile SCR applications, and computational fluid dynamics (CFD) has been widely used in the design optimization of spray nozzles, flow mixing characteristics, NO_x reduction processes, and urea decomposition (Thakur et al., 2003; Zheng et al., 2009; Zheng et al., 2010; Zhang et al., 2006; Zhang and Romzek, 2007; Birkhold et al., 2007; Nguyen et al., 2010; Larmi and Tiainen, 2003; Chen and Williams, 2005; Battoei et al., 2006). Thakur et al. (2003) provided an extensive review of static mixers in the processing industry, presenting guidelines for the selection of static mixers. Zheng et al. (2009) developed several types of mixers, including cone, 2-stage, and butterfly mixers. They also investigated the effect of in-pipe mixing devices on urea deposits with respect to mixer configurations and various exhaust gas temperatures. Zhang et al. (2006) introduced a simple flow mixer with twisted blades based on an original delta wing mixer for the purpose of creating both swirling and turbulent flows. Turbulent flow has a dominant effect on the flow mixing index or uniformity index in the short distance immediately behind the flow mixer (Zhang et al., 2006; Zhang and Romzek, 2007).

In allowing a sufficient mixing length by reducing the occupied space, it is necessary to develop a proper static mixer with a high mixing performance as well as a low pressure drop. However, there is insufficient research on the relationship between flow mixing characteristics and pressure drops in the marine engine fields.

In this study, both line- and swirl-type mixers were considered; each mixer was divided into three cases of vane angles: 30º, 45º, and 60º. The effects of a mixer's geometric structure on the flow mixing characteristics and the resulting pressure drop were investigated numerically using a commercial finite volume, three-dimensional (3-D) CFD code; FLUENT (version 6.3.26). The purpose of this study was to evaluate the effect of mixer geometry on the relative intensity, uniformity index, and pressure drop with the objective of enhancing the de-NO_x efficiency. Additionally, information pertaining to the selection of proper static mixers was provided based on the correlation between the uniformity index and the pressure drop.

NUMERICAL METHODS AND CONDITIONS

Analysis model

The geometry of the SCR system, which includes the position of the spray injector, mixer, SCR reactor, and measuring points, is shown in Fig. 1. Line-type and swirl-type mixers, as shown in Fig. 2, have 36 vanes each. A swirl-type mixer was developed in this study with several unique features: a simple design for production; a variable vane angle to generate different swirl flows; and the flexibility for installation and to control the mixer volume in the pipe. Both types of mixers with various vane angles were simulated in 3-D to investigate the flow pattern, turbulence characteristics, and uniformity of water, which is assumed to be UWS at the SCR catalyst entrance.

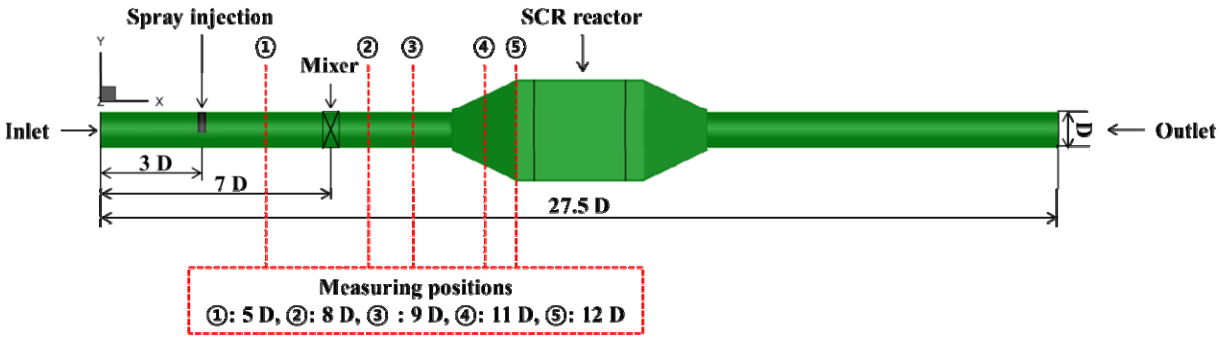

Fig. 1 Computational domain for the SCR system.

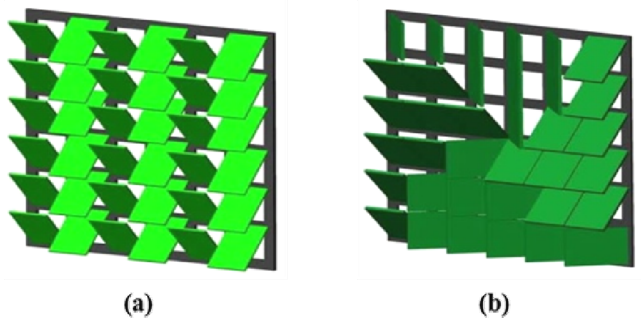

Fig. 2 Configuration of static mixers: (a) line-type mixer, and (b) swirl-type mixer.

The test conditions are listed in Table 1. The computational grid is composed of approximately 650,000 hexahedral and tetrahedral cells using FLUENT/GAMBIT (ANSYS, Inc., USA). The mesh structure became denser toward the spray injector and the mixer because of the high gradients of velocity, temperature, and species concentrations.

Table 1 Computational conditions with various mixer types and positions.

Case	Mixer type	Position of mixer and spray
1	W/O	7 D and 3 D from inlet boundary
2	Swirl, 30º	
3	Swirl, 45º	
4	Swirl, 60º	
5	Line (up-down), 45º	

Table 2 Summary of initial and boundary conditions.

Item	Section	Conditions and value
Boundary condition of computational domain	Inlet	Exhaust gas velocity: 20*m/s*, 573*K*
	Outlet	Pressure outlet: atmosphere
	Wall	Adiabatic / No-slip
	Catalyst	Porous media: $1/\alpha = 1.24 \times 10^7$, $C_2 = 10.59$
Initial condition of spray injection	Spray material	H_2O (liquid water), 300*K*
	Velocity	25*m/s*
	Angle	70º
	SMD: (Rosin-Rammler)	Mean diameter: 35μm, Spread parameter: 3.5
	Injection type	6 hole, solid cone type

Boundary conditions

The model assumes that the exhaust gas is fully developed and it consists of 77% N_2 and 23% O_2 by mass. A time step of 1*ms* was determined to be sufficient to produce results independent of the choice of time step. The injector consists of 6 holes with 0.45*mm* diameter. The initial and boundary conditions used in the calculation are shown in Table 2. The initial conditions of the exhaust gases were set based on full load and 900*rpm* on a 920*kW* diesel engine (HYUNDAI HiMSEN). The temperature of the exhaust gas was set to 573 *K*, and the inlet velocity was 20*m/s*.

Numerical procedure

The flow region in the SCR system is divided into three regions: the 1st region is the turbulent flow region in the upstream and downstream of the SCR reactor; the 2nd region is the laminar flow region in the SCR reactor; and the 3rd region is the region that contains the dispersed two-phase flow in the surrounding spray injector. The Lagrangian discrete phase model is used which contains sub-models for droplet dispersion, drag, and evaporation. An injection type of solid cone for primary breakup model is used to inject water liquid. To minimize computational time and stable convergence strategy, secondary breakup model for droplet breakup and collision are not considered in this study. The injected drop-size was found to follow a Rossin-Rammler distribution with a mean diameter of 35 microns and spread parameter of 3.5. For an incompressible, unsteady two-phase turbulent flow, the 3-D Reynolds-averaged Navier-Stokes (RANS) governing equations for mass, momentum, species concentration, and energy were solved. The standard κ-ε turbulent model was used to calculate the turbulent quantities. The continuity, momentum, and energy equations are expressed as follows in Eqs. (1)-(3), respectively.

$$\frac{\partial u_i}{\partial t} = 0 \tag{1}$$

$$\frac{\partial u_i}{\partial t} + \frac{\partial u_i u_j}{\partial x_j} = -\frac{\partial p}{\rho \partial x_i} + \frac{\partial}{\partial x_j}\left(\left(\nu + \nu_t\right)\left(\frac{\partial u_j}{\partial x_i} + \frac{\partial u_i}{\partial x_j} \right) \right) \tag{2}$$

$$\frac{\partial T}{\partial t} + \frac{\partial u_i T}{\partial x_i} = \frac{\partial}{\partial x_i} + \frac{\partial}{\partial x_j}\left(\left(\frac{\mu}{\mathrm{Pr}} + \frac{\mu_t}{\mathrm{Pr}_t} \right) + \frac{\partial T}{\partial x_i} \right) \tag{3}$$

The turbulent kinetic energy κ and the rate of energy dissipation ε are computed from a standard two-layer κ-ε turbulent model.

$$\frac{\partial \kappa}{\partial t} + \frac{\partial u_i \kappa}{\partial x_i} = \frac{\partial}{\partial x_j}\left(\left(\nu + \frac{\nu_t}{\sigma_\kappa} \right) \frac{\partial \kappa}{\partial x_i} \right) + G - \varepsilon \tag{4}$$

$$\frac{\partial \varepsilon}{\partial t} + \frac{\partial u_i \varepsilon}{\partial x_i} = \frac{\partial}{\partial x_j}\left(\left(\nu + \frac{\nu_t}{\sigma_\varepsilon} \right) \frac{\partial \varepsilon}{\partial x_i} \right) + \frac{\varepsilon}{\kappa}\left(C_{\varepsilon 1} G - C_{\varepsilon 2} \varepsilon \right) \tag{5}$$

G denotes the production rate of κ and is given below:

$$G = -\overline{u_i u_j} \frac{\partial u_i}{\partial x_j} = \nu_t \left(\frac{\partial u_i}{\partial x_j} + \frac{\partial u_j}{\partial x_i} \right) \frac{\partial u_i}{\partial x_j}, \text{ and } \quad \nu_t = C_\mu \frac{\kappa^2}{\varepsilon} \tag{6}$$

In the above equations, the coefficients are as follows:

$$C_{\varepsilon 1} = 1.44, \quad C_{\varepsilon 2} = 1.92, \quad C_\mu = 0.09, \quad \sigma_\kappa = 1.0, \text{ and } \quad \sigma_\varepsilon = 1.3.$$

The catalyst is the core of SCR reactor. In this study, a honeycomb type SCR catalyst filter was adopted. If the catalyst filter is constructed physically from a numerical simulation without any simplifications, the grid of the model will reach a level that is beyond the calculation capabilities of most computing systems. Therefore, an approach of a porous media model was adopted

to simulate the flow in the catalyst filter. The mass and momentum transfer in the radial direction was ignored because the axial velocity is dominant in the SCR filter (Jeong et al., 2005). In this simple model, the pressure change (drop) is defined by a combination of Darcy's Law and an additional inertial loss term along the SCR filter (Fluent, 2007):

$$\Delta p = -\left(\frac{\mu}{\alpha} v + C_2 \frac{1}{2} \rho v^2 \right) \Delta m \tag{7}$$

$$p = 2.73v^2 - 199.72v \tag{8}$$

where Δp is the pressure drop, μ is the laminar fluid viscosity, α is the permeability of the medium, C_2 is the pressure-jump coefficient, v is the velocity normal to the porous face, and Δm is the thickness of the medium. To obtain the two unknown values, α and C_2, a quadratic equation of Eq. (8) is derived from the calculation of the simple part cell analysis as shown in Fig. 3. Appropriate values for α and C_2 can be calculated using Eqs. (7) and (8) as shown in Table 2.

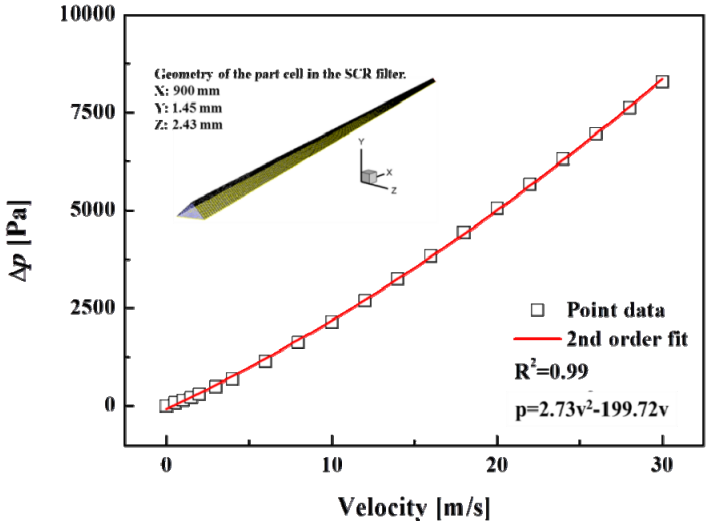

Fig. 3 Pressure drop distribution of the part cell in the SCR filter with respect to inlet bulk velocity.

RESULTS AND DISCUSSION

Distributions of velocity and water mass fraction in SCR system

Fig. 4 illustrates the contours of the velocity and water concentration of parts of the SCR system, including the spray injector, mixer, and reactor. Case 1 represents the calculation conditions of no mixer. Cases 2, 3, and 4 represent the calculation conditions of swirl-type mixers with vane angles of 30º, 45º, and 60º, respectively. Case 5 represents the calculation conditions of a line-type mixer with a vane angle of 45º. Considerable disturbances occur surround the spray injector for all cases. The flow patterns behind the mixers differ with the mixer type. In the swirl-type mixers of cases 2, 3, and 4, the central recirculation zone (CRZ) is generated near the mixer fields, and the CRZ increases with increasing vane angle. The line-type mixer, however, does not exhibit a CRZ, because the main flow near the mixer moves up and down. The velocity distribution and water concentration of case 1 in front of the SCR reactor are concentrated in the center region. This phenomenon may promote serious problems, such as catalyst filter damage and NH_3 slip (NMRI, 2011). For the remainder of the cases (cases 2-5), the velocity and concentration of water are relatively well distributed in comparison to case 1. In particular, Fig. 4(b) demonstrates that the mass fraction of water for case 3 appears well mixed with input gases in front of the SCR reactor. Based on these results, NH_3 slip, low mixing of UWS with hot exhaust gases, and catalyst filer damage in front of the SCR reactor have the potential to be mitigated without using any guide vanes, such as baffles.

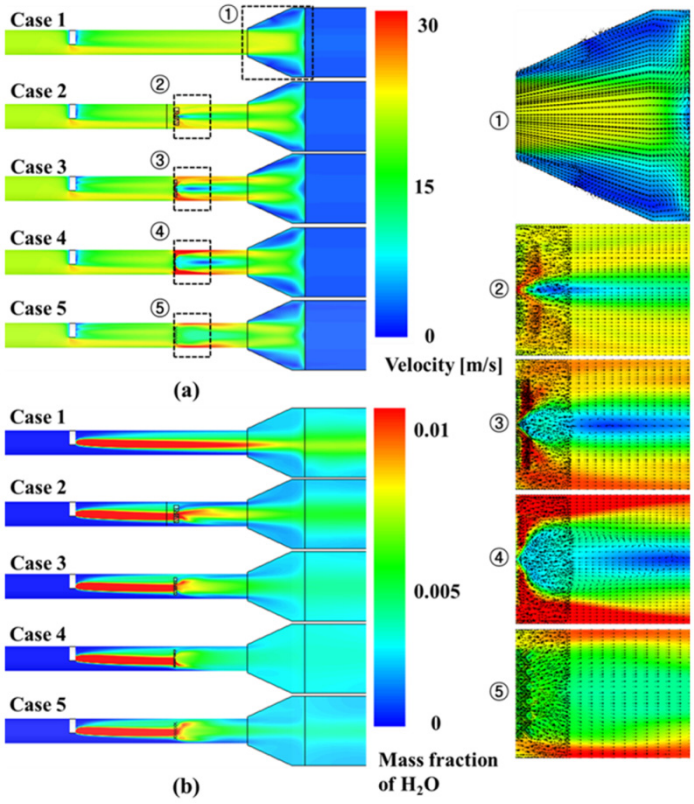

Fig. 4 Contours of (a) velocity and (b) water concentration for different cases with a calculation time 1.5*s*.

Effect of mixer geometry on turbulent flow characteristics

Turbulent flow occurs when instabilities in a flow are not sufficiently damped by viscous action and the fluid velocity at each point in the flow exhibits random fluctuations (Turns, 2000). Turbulence can be depicted as fluctuations in a fluid flow. When working with chemicals as in an SCR reactor, typically a high level of flow fluctuations is preferable for the mixing of UWS with exhaust gases. It is common to define the relative turbulent intensity for the velocity as follows:

$$TI = \frac{u'}{\bar{U}} \tag{9}$$

where u' is the root-mean-square (RMS) of the turbulent velocity fluctuations ($U - \bar{U}$) at a particular location over a specified period of time, and $\bar{U}$ is the average of the velocity for the instantaneous value (U) at the same location over the time period. For the same theory, the standard deviation of the temporal variation of Reynolds averaged velocity (σ) and its relative intensity ($RI = \sigma / \bar{U}$) are adopted. In this RANS simulation, $U - \bar{U}$ is the temporal variation of Reynolds averaged velocity, not the turbulent velocity fluctuations because U represents the Reynolds averaged velocity.

Fig. 5 shows σ for 0.3*s* for different measuring positions and mixer geometries. For case 1 (no mixer), there were few changes in velocity at positions 1, 2, and 3. However, σ significantly increased near the SCR filter because a large recirculation zone formed in the diffuser region. When the flow enters the porous zone, it aligns with the channel direction and the higher pressure is located around the catalyst entrance and the center line (Chen et al., 2004). The results of all cases at positions 4 and 5 exhibit a similar tendency. At position 5, σ for all cases is relatively lower than that at positions 2, 3, and 4. Case 4 has the highest σ after the mixer owing to a large CRZ. This behavior can be explained as a result of the vorticity magnitude generated by the induced flow direction of the mixers. Vorticity is a measure of the rotation of a fluid element as it moves in a field, and is defined as the curl of the velocity vector:

$$\omega = \nabla \times \mathbf{V} \tag{10}$$

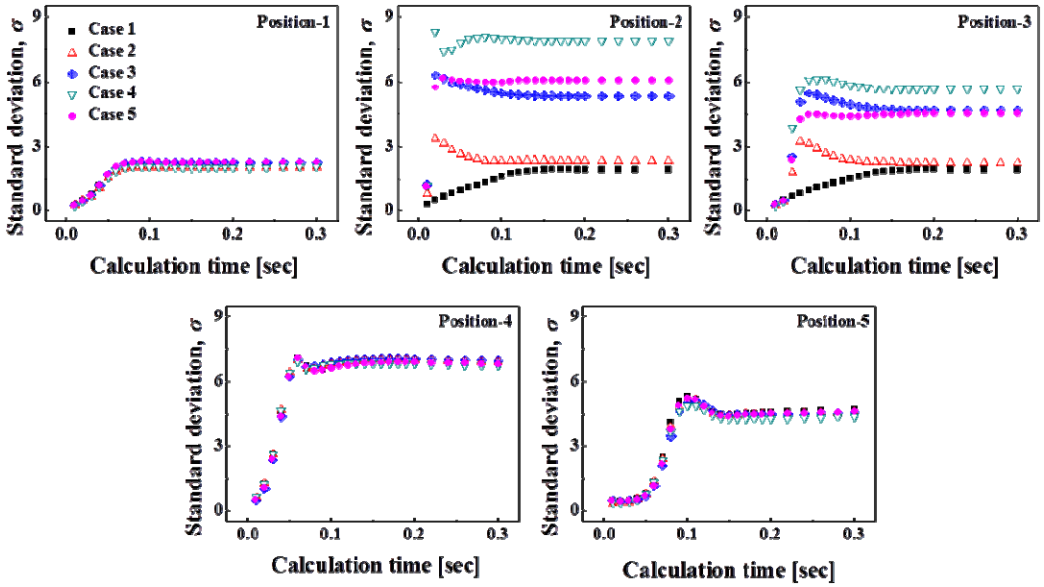

Fig. 5 History of the standard deviation (σ) up to 0.3s for different measuring points and different cases.

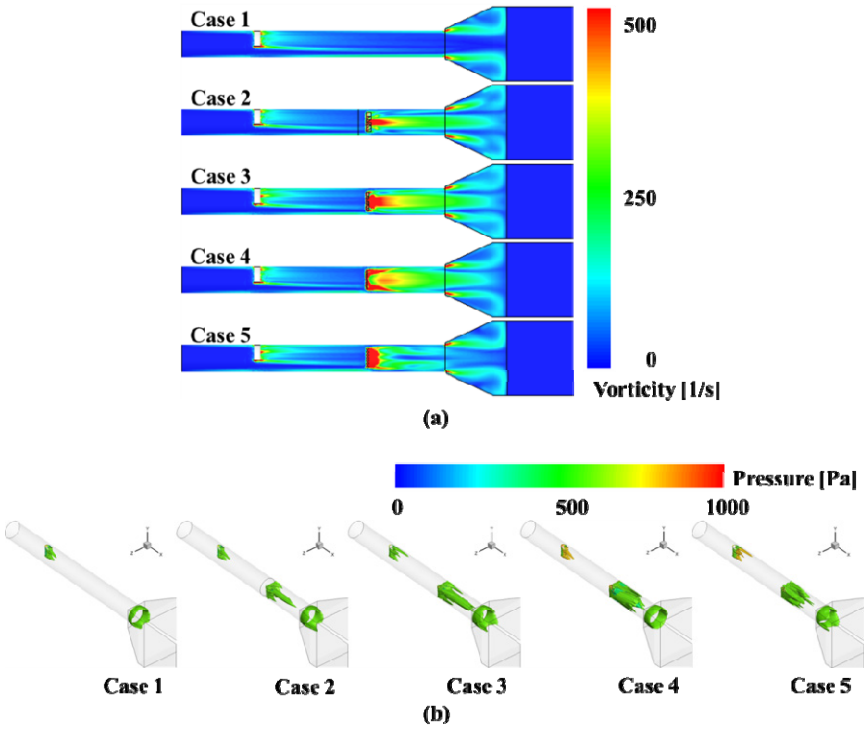

Fig. 6 Contours of different cases of (a) vorticity magnitude and the iso-surface of vorticity at 500 1/s and (b) pressure, both obtained with a calculation time of 1.5s.

Fig. 6 shows the contours of the vorticity magnitude and the iso-surface of the vorticity magnitude for all cases. Except for case 1, the other cases exhibit a high vorticity magnitude regardless of the mixer type. This is because the introduced flow is concentrated at the center region for the case 1, while the line-type and swirl-type models disperse the flow to the wall. For case 5 (line-type mixer), the vorticity magnitude was relatively high by the turbulent flow immediately behind the mixer. A small-scale vortex may be generated directly behind the mixer, and vanishes rapidly after passing through it. For the swirl-type mixers, the vorticity magnitude is longer with stream-wise axis than that for the line-type mixer. In addition, the volume of the vorticity as shown in Fig. 6 increases because the CRZ gradually increases with the vane angle. The results above indicate that the size and length of the CRZ are controlled by the mixer shape. The swirl-type mixer creates both turbulent and

swirling flows. Therefore, it is important to select the appropriate mixer in order to maximize flow mixing and minimize NH_3 slip. The reaction for NO_x reduction in SCR catalysts requires a sufficient reaction time within a certain temperature range. The NO and the NH_3 do not react at lower temperatures and insufficient flow mixing. NH_3 slip is a means of NH_3 passing through the SCR reactor un-reacted.

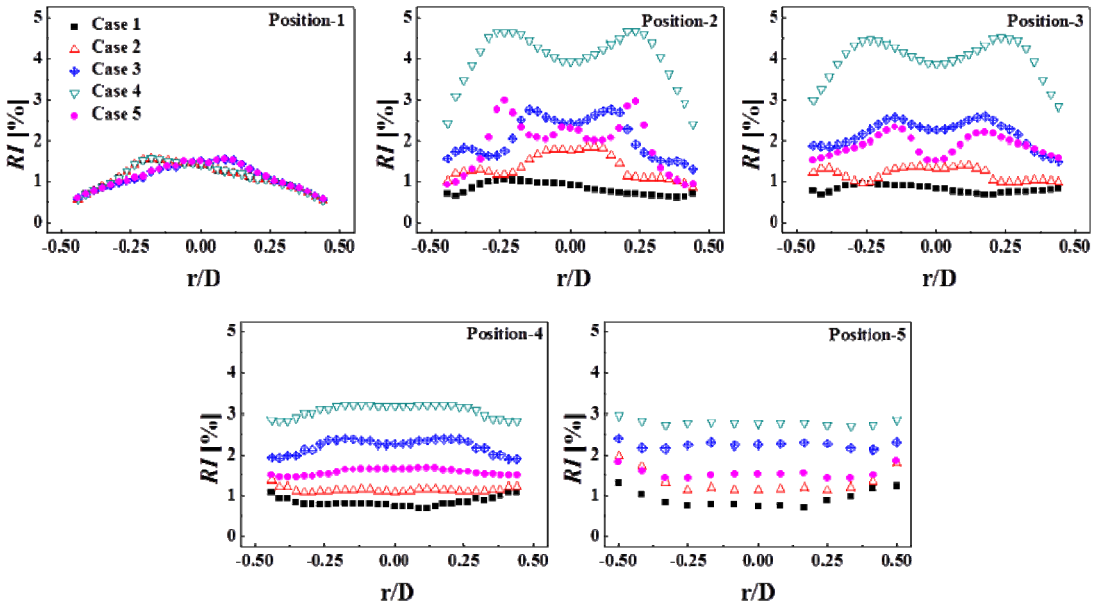

Fig. 7 Distributions of relative intensity (*RI*) for different measuring points and cases using a calculation time of 1.5*s*.

Fig. 7 presents relative intensity (*RI*) distributions at 1.5*s* for different measuring positions and mixer geometries. In all mixer cases, there are relatively small changes in the *RI* at position 1. *RI* substantially increases at position 2 after passing through the mixers. After this point, *RI* gradually decreases, and exhibits uniform distributions as it approaches the SCR filter. The maximum *RI* values were as follows: 1.54% at position 1 for case 1, 1.96% at position 5 for case 2, 2.75% at position 2 for case 3, 4.67% at position 2 for case 4, and 2.99% at position 2 for case 5. Incorporating the mixer is most effective for improving mixing performance immediately behind the mixer when the vane angle is greater than 45º. Although case 4 possesses the highest *RI* for all measuring positions, the levels of the mean *RI* for case 3 are constantly maintained along the stream-wise axis from measuring positions 2 to 3 as shown in Fig. 8. From an operational point of view with respect to the durability and the likelihood of system failure, case 3, a swirl-type mixer with a 45º vane angle, is more favorable than other cases.

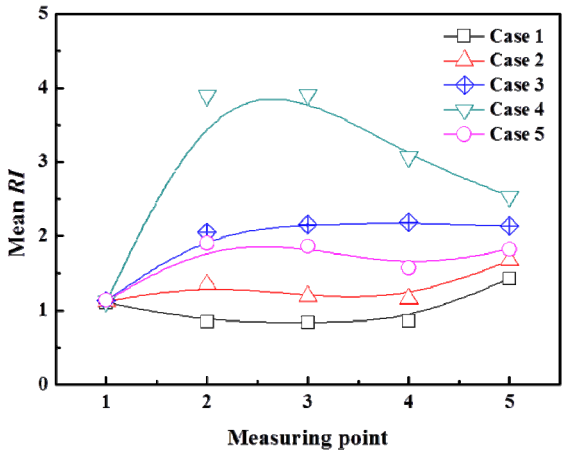

Fig. 8 Distributions of mean *RI* with respect to measuring points for different cases using a calculation time of 1.5*s*.

Relationship between pressure drop and uniform flow

A uniform flow and UWS distribution across the front of the catalyst filter are necessary to obtain a maximum performance for de-NO_x and a minimum NH_3 slip in the SCR system. The flow uniformity index is a commonly used indicator of the flow distribution degree for after-treatment applications (Weltens et al., 1993; Bressler et al., 1996; Girard et al., 2006). In this study, a similar definition is adopted to evaluate the distribution degree of water concentration at a certain location along the pipe:

$$UI_c = 1 - \frac{1}{2n}\sum_{i=1}^{n}\frac{\sqrt{\left(C_i - \overline{C}\right)^2}}{\overline{C}} \tag{11}$$

where, UI_c is the uniformity index for the water concentration, C_i is the local concentration of water, $\overline{C}$ is the average concentration of water, and n is the number of cells. Generally, higher UI_c indicates better fluid mixing.

Fig. 9 shows the UI_c with respect to the calculation time (from 0.3 to 1.5s) for the stream-wise positions 1 to 5 and for cases 1 to 5. The effects of the mixer on the UI_c are quite strong, regardless of the type of mixer. Compared to case 1, the cases with mixers improve the UI_c by approximately 20% in positions 2 and 3, approximately 30% in the position 4, and approximately 5% in position 5. For all cases, the UI_c increased along the stream-wise direction. The maximum values of the UI_c were 98.5% for case 4, 96% for case 3, 94% for case 2, 93.6% for case 5, and 90% for case 1. The sequences for the UI_c at different position are as follows: case 3 > case 5 > case 1 > case 4 > case 2 before the mixer at the position 1; case 4 > case 5 > case 3 > case 2 > case 1 behind the mixer at the position 2; case 4 > case 3 > case 5 > case 2 > case 1 at positions 3 and 4; and case 4 > case 3 > case 2 > case 5 > case 1 in the right front of the catalyst filter at the position 5. These results indicate that the UI_c increases with increase in the vane angle of the swirl-type mixer, and the cases for the swirl-type mixer generally show better mixing performance than the line-type mixer, even though the line-type mixer outperforms it behind the mixer and in the region of the diffuser. This superior performance is due to a small-scale vortex generated by the up and down induced flow behind the line-type mixer that vanishes rapidly in a short region. Conversely, for the swirl-type mixer, a large-scale vortex in terms of CRZ is generated in a long region. Therefore, obtaining a certain distance to mix of the UWS with the exhaust gases is important, and the swirl-type mixer is better than the line-type mixer with respect to uniform flow and the higher mixing performance in practical SCR applications.

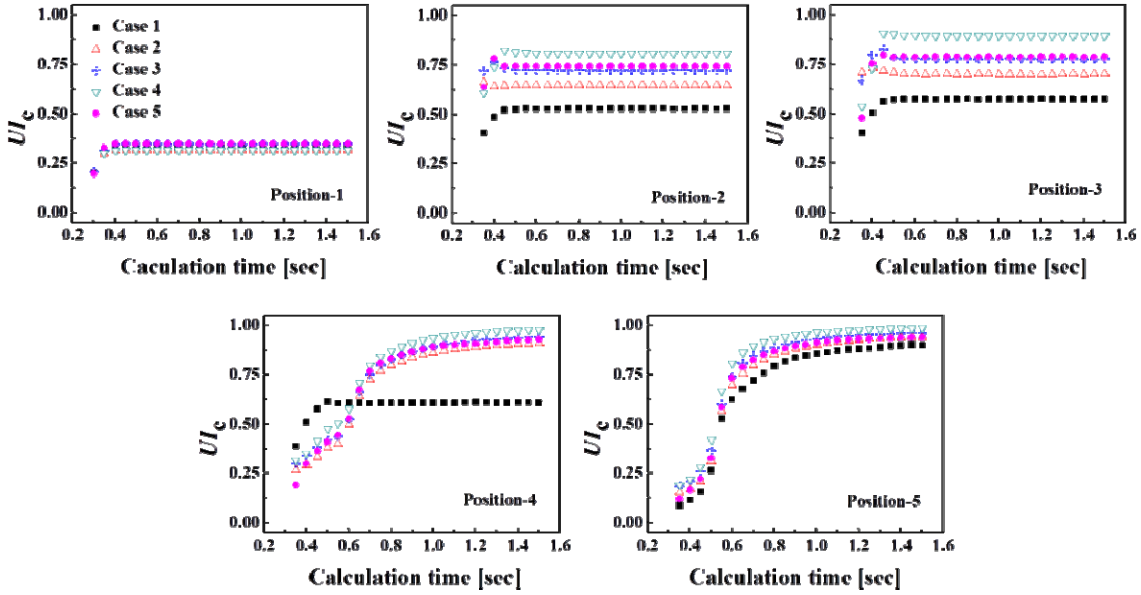

Fig. 9 History of uniformity index (UI_c) for H_2O from 0.3 to 1.5s for different measuring points and cases.

Mixer development generally focuses on the high efficiency of NO_x reduction because of its direct impact on the design target; however, it is difficult to determine the total performance of mixing devices based on only the UI_c. A more thorough understanding of the flow pattern characteristics and pressure drop is helpful in designing an SCR system with optimal performance for both NO_x reduction and system durability. Fig. 10 depicts the relationship between the UI_c and pressure drop for different cases. As expected, the case 1 has the lowest pressure loss and UI_c, which are 647 Pa and 90%, respectively. The presence of any type of mixer resulted in an improved flow mixing, but a penalty of additional pressure loss. Case 4 had the best mixing performance although the pressure drop was the worst. There is a tradeoff relationship between the UI_c and the pressure drop with increasing vane angle for swirl-type mixers. Case 5 has a higher UI_c and a pressure drop than case 1. However, the UI_c is lower and pressure drop is higher than those for the swirl-type mixers (cases 2-4) at the position 5, as shown in Fig. 9. Furthermore, in a comparison of case 3 and 5, which contain the same angle of 45, case 3 shows higher UI_c and a lower pressure drop than case 5, as shown in Fig. 10. Therefore, it is concluded that the swirl-type mixer is more effective than the line-type mixer with respect to the enhancement of UI_c and *RI*. When selecting a static mixer in SCR applications, it is necessary to consider the mixing and the uniform distribution of the UWS in front of the SCR reactor as well as the pressure drop, which is not desirable for the optimization of engine power throughout the system. Finally, it can be concluded that the swirl-type mixer with a vane angle of 45 is more suitable model in this study based on the results of mean *RI*, UI_c and pressure drop. Further research focused on the effect of the vane size becoming larger or smaller may be needed under line- and swirl-type mixers. The effectiveness of swirl-type mixers is carefully guessed to be initiated from the larger-scale swirl than those of line-type mixers. It is because the line-type mixer is able to generate the vane-scale swirls whereas the duct-scale swirl is produced by the swirl mixer. Nevertheless, this study may provide useful information for selecting a static mixer in SCR applications.

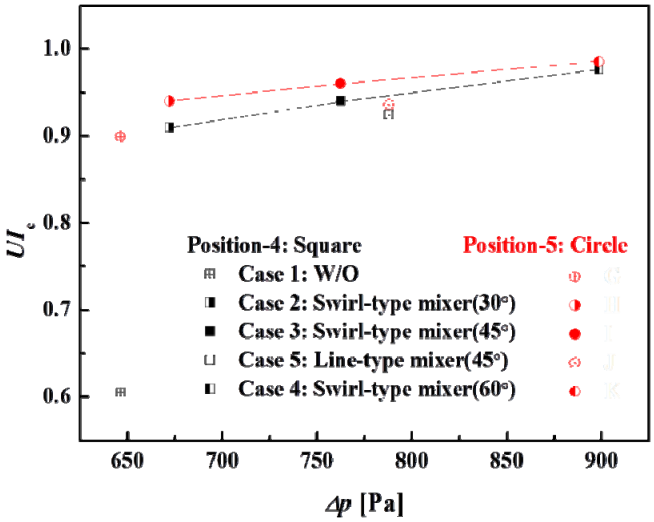

Fig. 10 Relationship between uniformity index and pressure drop for different cases with a calculation time of 1.5*s*.

CONCLUSIONS

3-D numerical simulations were performed to investigate the effects of mixer geometry on the mixing performance and the pressure drop. Flow mixing and uniformity can be greatly improved by using a static mixer in the SCR system. Turbulent and swirling flows can also achieve a great improvement for flow mixing with respect to flow recirculation phenomena through a longer distance. In this study, information regarding the selection of proper static mixers was provided based on the correlation between the uniformity index and the pressure drop. The results show that the mixer for SCR applications can be effectively optimized by using a well-designed mixing device. The main results are summarized as follows:

1) In comparison to the case without a mixer, the cases with a mixer improve the uniformity index by approximately 20% directly behind the mixer, approximately 30% in the diffuser, and approximately 5% immediately in front of the mixer.
2) In the swirl-type mixer, the CRZ is generated directly behind the mixer, and increases with the vane angles of the mixer. Therefore, it is expected that the mixing region is longer with stream-wise axis because the swirl-type mixer creates turbulent and swirling flows.
3) The swirl-type mixer is more effective than the line-type mixer with respect to the enhancement of mixing performance, even though there is a tradeoff relationship between the uniformity index and the pressure drop. Therefore, the swirl-type mixer with a vane angle of 45º is the most suitable model in this study based on the results of both parameters.

ACKNOWLEDGEMENTS

This work was supported by the National Research Foundation of Korea (NRF) grant funded by the Korea government (MEST) through GCRC-SOP and this work was supported by the Human Resources Development program (No. 20124010-203230-11-1-000) of the Korea Institute of Energy Technology Evaluation and Planning (KETEP) grant funded by the Korea government Ministry of Trade, Industry and Energy.

REFERENCES

Battoei, M., Doroudian, M. and Lacin, F., 2006. *Optimization of exhaust gas distribution on the catalytic converter inlet-cone diffuser using advanced shape deformation technology, SAE Technical Paper*, 2006-01-1439, Pennsylvania: 4 SAE International.

Birkhold, F., Meingast, U., Wassermann, P. and Deutschmann, O., 2007. Modeling and simulation of the injection of urea-water-solution for automotive SCR $DeNO_x$-systems. *Applied Catalysis B : Environmental*, 70, pp.119-127.

Bressler, H., Rammoser, D., Neumaier, H. and Terres, F., 1996. *Experimental and predictive investigation of a close coupled catalytic converter with pulsating flow, SAE Technical Paper*, 960564, Pennsylvania: 4 SAE International.

Chen, M. and Williams, S., 2005. Modelling and optimization of SCR-exhaust aftertreatment systems. *SAE Technical Paper*, 2005-01-0969, Pennsylvania: 4 SAE International.

Chen, M., Aleixo, J., Williams, S., Leprince, T. and Yong, Y., 2004. *CFD modeling of 3-way catalytic converters with detailed catalytic surface reaction mechanism. SAE Technical Paper*, 2004-01-0148, Pennsylvania: 4 SAE International.

DieselNet, 2008. *Emission Standards, IMO Marine Engine Regulations*. [online] Available at: <http://www.dieselnet.com/standards/inter/imo.php > [Accessed March 2013].

Fluent, 2007. *Fluent 6.3 User's Guide.* Lebanon: ANSYS Inc.

Girard, J. W., Lacin, F., Hass, C.J. and Hodonsky, J., 2006. *Flow uniformity optimization for diesel aftertreatment systems, SAE Technical Paper*, 2006-01-1092, Pennsylvania: 4 SAE International.

Jeong, S.J., Lee, S.J., Kim, W.S. and Lee, C.B., 2005. *Simulation on the optimization shape and location of urea injecttion for urea-SCR system of heavy-duty diesel engine to prevent NH_3 slip, SAE Technical Paper*, 2005-01-3886, Pennsylvania: 4 SAE International.

Larmi, M. and Tiainen, J., 2003. *Diesel spray simulation and KH-RT wave model, SAE Technical Paper*, 2003-01-3231, Pennsylvania: 4 SAE International.

Munnannur, A. and Liu, Z. G., 2010. *Development and validation of a predictive model for DEF injection and urea decomposition in model SCR deNO_x systems, SAE Technical Paper*, 2010-01-0889, Pennsylvania: 4 SAE International.

Nguyen, T.D.B., Lim, Y.I., Eom, W.H., Kim, S.J. and Yoo, K.S., 2010. Experimental and CFD simulation of hybrid SNCR-SCR using urea solution in a pilot-scale reactor. *Computers and Chemical Engineering*, 34(10), pp.1580-1589.

NMRI, 2011. *National Maritime Research Institute 2011*. [online] Available at: <http://www.nmri.go.jp/main/panfuretto/content/pamphlet2011_e.pdf > [Accessed November 2013].

Regner, M., Östergren, K. and Trägårdh, C., 2006. Effect of geometry and flow rate on secondary flow and the mixing process in static mixers-A numerical study. *Chemical Engineering Science*, 61(18), pp.6133-6141.

Thakur, R.K., Vial, Ch., Nigam, K.D.P., Nauman, E.B. and Djelveh, G., 2003. Static mixers in the process industries-A review. *Chemical Engineering Research and Design*, 81(7), pp.787-826.

Turns, S.R., 2000. *An Introduction to combustion: concept and applications*. 2nd ed. Boston: McGraw-Hill.

Weltens, H., Bressler, H., Terres, F., Neumaier, H. and Rammoser, D., 1993. *Optimization of catalytic converter gas flow distributions by CFD prediction, SAE Technical Paper*, 930780, Pennsylvania: 4 SAE International.

Zhang, X. and Romzek, M., 2007. *3-D numerical study of flow mixing in front of SCR for different injection systems*, *SAE Technical Paper*, 2007-01-1578, Pennsylvania: 4 SAE International.

Zhang X., Romzek, M. and Morgan, C., 2006. *3-D numerical study of mixing characteristics of NH_3 in front of SCR, SAE Technical Paper*, 2006-01-3444, Pennsylvania: 4 SAE International.

Zheng, G., Fila, A., Kotrba A. and Floyd, R., 2010. *Investigation of urea deposits in urea SCR systems for medium and heavy duty trucks, SAE Technical Paper*, 2010-01-1941, Pennsylvania: 4 SAE International.

Zheng, G., Palmer, G., Salanta G. and Kotrba, A., 2009. *Mixer development for urea SCR application, SAE Technical Paper*, 2009-01-2879, Pennsylvania: 4 SAE International.